ACS APPLIED MATERIALS & INTERFACES

Research Article

www.acsami.org

Sustained Release of Heparin on Enlarged-Pore and Functionalized MCM-41

Mi Mi Wan, Jia Yuan Yang, Yue Qiu, Yu Zhou, Chen Xi Guan, Qian Hou, Wei Gang Lin, and Jian Hua Zhu*

Key Laboratory of Mesoscopic Chemistry of MOE, College of Chemistry and Chemical Engineering, Nanjing University, Nanjing 210093, China

Supporting Information

ABSTRACT: Mesoporous silica MCM-41 and SBA-15 were chosen to study the adsorption and release of bulky biomolecule heparin, in order to develop new heparin controlled delivery system and expand the application of mesoporous materials in life science. To explore how the structure of support such as pore size and surface state affects the accommodation and release of heparin, we used decane as swelling agent to enlarge pores of MCM-41, introduced amino groups for improving the biocompatibility of support, and controllably retained templates in the as-synthesized sample. The influence of modification on the structure of samples was investigated by XRD and N_2 adsorption−desorption, whereas their performance of adsorbing and releasing heparin was assessed with that of toluidine blue method. Both enlarged pore and organic modification significantly promoted the adsorption and prolonged the release of heparin in MCM-41, and the release was characterized with a three-stage release model. The mechanism of heparin release from mesoporous material was studied by fitting the release profiles to the theoretical equation. As expected, some mesoporous composites could release heparin in the long term with tuned dosage.

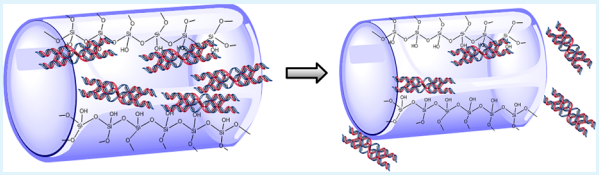

KEYWORDS: *mesoporous silica, heparin, adsorption, controlled release, pore-enlarging, organic modification*

1. INTRODUCTION

Heparin is a highly sulphated linear polysaccharide existing in the granules of mast cells and the granulated cells of organs such as liver and intestine.[1] This compound can prevent proliferation, enhance biocompatibility, and is often used as a powerful anticoagulant.[2,3] Heparin also mediates a range of biological and physiological activities such as anticoagulation,[4] complement activation,[5,6] vascular regeneration,[7,8] antiviral activity,[9−11] and release of lipoprotein lipase and hepatic lipase.[12] For these reasons, heparinization becomes an efficient way to enhance the performance of blood-containing artificial biomaterials.[13−17] Among various methods to introduce heparin, injection can effectively inhibit the formation of thrombus,[4,18] but it increases the possibility of hemorrhage at the same time. Heparinizing the scaffolds to guarantee their hemocompatibility can prevent thrombus during surgeries, but it is hard to maintain the required concentration of heparin in fast blood flow for a long period. Common heparinization methods such as ion-bonding, end-point attachment and covalent-bonding hardly guarantee the controlled release of heparin because of the too strong or weak bond energies.[19] For instance, covalent chemical adsorption can greatly improve the stability of heparin in the vessel but lowers its activity at the same time.[13,17,20] Recently, research has focused on encapsulating heparin in functional materials and manipulating the drug concentration through controlled release. These functional materials include capsule, some hydrogels, biological molecules, and so on.[21−23] However, there still remain many limitations on the long-term release of heparin.

Polymers and macromolecules are promising candidates for drug-controlled delivery.[24,25] Nonetheless, their disadvantages such as low mechanical strength, poor chemical stability, unsatisfactory biocompatibility, and even some toxicity inhibit their actual applications.[4] Some synthesized polymers induce inflammation or intimal hyperplasia in animal models,[26,27] and many polymers are nonbiodegradable so that additional surgeries are required to remove them, which bring patients great pains.[4] Consequently, inorganic materials become another choice for drug delivery, and among them, silica molecular sieves have attracted the growing attention because of their facile structure control, surface functionalization and good biocompatibility.[28−31] The drugs adsorbed in the long and narrow channels will undergo a long diffusion distance to pore entrance, which is beneficial for avoiding the rapid release. Furthermore, the adsorption and release performance of mesoporous materials can be controlled by tailoring their composition, pore configuration and surface state.[32−35] Thereby, mesoporous silica and its organic-modified analogue[25,36,37] have been tried in the delivery of some drugs. Our preliminary research on the release of heparin from vascular prosthesis containing mesochannels also showed a positive result.[38]

Received: May 17, 2012
Accepted: July 31, 2012
Published: July 31, 2012

   dx.doi.org/10.1021/am300878z | ACS Appl. Mater. Interfaces 2012, 4, 4113−4122

Table 1. Textural Properties and Heparin Release Ability of MCM-41 and SBA-15 Series Samples[a]

samples	decane to CTAB	APTES to silica	S_{BET} (m^2 g^{-1})	S_{mic} (cm^2 g^{-1})	V_p (cm^3 g^{-1})	V_{mic} (cm^3 g^{-1})	D_{BJHp} (nm)	adsorbed heparin (mg g^{-1}, A)	released after 60 days (mg g^{-1}, B)	B/A
SBA-15	0	0	902	187	1.09	0.08	6.3	24.6 ± 3	21.6[b]	0.88
SBA-15-r	0	0	788	38	1.14	0.005	6.2	34.6 ± 4.5	14.2[b]	0.41
MCM-41	0	0	1118	0	0.94	0	2.4	14.6 ± 1.8	10.0[b]	0.69
MCM-41-r	0	0	780	0	0.41	0	1.7	65.1 ± 8	25.1[b]	0.39
ML-1	0.25	0	1163	17.0	1.19	0	3.0	42.6 ± 5.5	20.1	0.47
ML-2	0.5	0	1147	34.1	1.18	0	3.1	42.2 ± 5	24.9	0.59
ML-3	1.0	0	1056	62.2	1.23	0.013	4.5	54.3 ± 7	38.6	0.71
ML-3[c]	--	--	473	101	0.36	0.04	3.6			
ML-3-r	1.0	0	592	0	0.72	0	3.8	74.0 ± 9	25.1[b]	0.34
ML-4	1.5	0	1072	56.9	1.25	0.010	4.5	49.4 ± 0.6	28.8	0.58
ML-5	2.0	0	1073	86.7	1.27	0.024	4.5	48.7 ± 6	29.4	0.60
ML-6	2.5	0	1105	68.5	1.28	0.015	4.5	44.7 ± 5.8	27.3	0.61
ML-3a	1.0	0.05	633	0	0.79	0	3.7	52.3 ± 6.7	9.2	0.18
ML-3a[c]			350	0	0.4	0	3.6			
ML-3b	1.0	0.07	723	0	0.89	0	3.8	60.3 ± 7.8	19.1	0.32
ML-3c	1.0	0.10	630	0	0.76	0	3.8	80.4 ± 10	13.2	0.16
ML-3d	1.0	0.20	402	0	0.70	0	3.9	99.5 ± 13	39.5	0.40

[a] S_{BET} is the BET surface area, V_p is the total pore volume, D_{BJH} is obtained according to the maximum of the KJS pore size distribution calculated from the adsorption branch of the isotherm. [b] Release amount of total adsorbed heparin after the 30 days' release. [c] Samples after heparin immobilization.

However, how the pore size of mesoporous silica affects the accommodation and release of the bulky biomolecule heparin is still inexplicit and detailed study is required. For this purpose, two mesoporous silica materials MCM-41 and SBA-15 were used here to adsorb and release heparin. Especially the MCM-41 with enlarged pore is emphatically studied, and the positively charged amino groups were chosen as the organic modifier to promote the adsorption of heparin and prolong the release time, since it has been reported that this modifier promoted enzyme immobilization on mesoporous silica significantly.[39−41] Lastly, templates are controllably retained in the as-synthesized sample in order to promote the immobilization and release of the biomolecule in mesoporous silica with the assistance of retained template.[41]

2. EXPERIMENTAL SECTION

2.1. Materials and Reagents. Cetyltrimethylammonium bromide (CTAB) and silica aerosol were produced by Nanjing Chemical Reagents and Qingdao Haiyang (China), while TEOS (Tetraethylorthosilicate) and P123 ($EO_{20}PO_{70}EO_{20}$) were purchased from Shanghai Wulian (China) and Aldrich, respectively.

Fabrication of MCM-41 was performed according to literatures.[42] Silica aerosol (3 g) was added to NaOH solution (0.5 M, 45 mL) under stirring and heated at 333 K to dissolve, and then a solution (25 mL) containing CTAB (4.5 g) was added into the mixture dropwise under stirring. The pH value of the mixture was adjusted to 11.5 using HCl solution (2 M), and the gel mixture was heated statically at 403 K for 72 h after stirring of 6 h. Finally, the solid product was recovered by filtration, washed with distilled water, and air-dried to give the as-MCM-41 sample. Part of the product was calcined at 823 K for 5 h in air to obtain the template-free sample denoted as MCM-41, while 1 g of the as-MCM-41 was refluxed with 200 mL ethanol to get MCM-41-r sample, in order to retain part of CTAB template inside the channel.[41]

To obtain the enlarged-pore MCM-41, the calculated amount of decane[43] was added into the solution of CTAB under vigorous stirring for 1 h once the CTAB was absolutely dissolved in the process mentioned above. Subsequently, the mixture was dropwise added to the silica source solution, and then the pH value was tuned to 10 with HCl solution (2M). The succeeding synthetic process was the same as that of normal MCM-41, giving the product named as-ML-n (n = 1, 2, 3, 4, 5, 6), where n differentiates the molar ratio of decane to CTAB (Table 1). Similarly, part of the as-ML-n was calcined to obtain ML-n samples. Meanwhile, ML-3-r sample was gained by refluxing 1.0 g of the as-synthesized material in 200 mL ethanol for 24 h, as mentioned above.

The organic modification of ML-3 was carried out by semidirect synthesis method:[44] After the synthetic mixture of ML-3 was adjusted by its pH value and stirred for 2 h, a given amount of 3-aminopropyltriethoxysilane (APTES) was added and stirred for another 4 h, following the same succeeding process to give as-ML-3x samples (x = a, b, c, d), where x represents the different molar ratio of APTES to silica used in synthesis (Table 1). One gram of the sample was refluxed with 200 mL of ethanol containing 1.5 mL of HCl and to obtain ML-3x composite.

Synthesis of SBA-15 was according to literature.[33,45] In a typical synthesis, 2 g of P123, 60 g of HCl (2 mol L^{-1}), and 15 g of water were mixed at room temperature. Once P123 was dissolved in the solution, 4.25 g of TEOS were added at 313 K under vigorous stirring for 24 h, and then the mixture was heated statically at 373 K for 24 h. The solid product was recovered by filtration, washed by distilled water, air-dried, and named as-SBA-15. Parts of as-SBA-15 were calcined in air at 823 K for 5 h to get SBA-15 sample, whereas SBA-15-r sample was obtained by refluxing 1.0 g of the as-synthesized material in 200 mL ethanol for 24 h to partly remove the template.[41]

2.2. Methods. The X-ray diffraction (XRD) patterns were recorded on an ARL XTRA diffractometer with Cu Kα radiation in the 2θ range from 0.5 to 8°.[44] Nitrogen adsorption and desorption isotherms were measured at 77 K by using a Micromeritics ASAP 2020 volumetric adsorption analyzer, and about 100 mg of samples were evacuated at 573 K for 4 h in the degas port of the analyzer prior to test. The organosilane-functionalized samples were evacuated at 373 K for 5 h before measurements.[44] The Brunauer−Emmett−Teller (BET) specific surface area was calculated using adsorption data in the relative pressure range from 0.04 to 0.2, and the total pore volume of sample was determined from the amount adsorbed at a relative pressure of about 0.99, whereas the pore size distribution curves were calculated from the analysis of the adsorption branch of the isotherm using the Barrett−Joyner−Halenda (BJH) algorithm. The primary mesoporous volume, V_p, and microporous volume of sample, V_{mic}, were calculated by the t-plot method. Thermogravimetric and differential scanning calorimetric (TG-DSC) analysis was performed on a NETZSCH

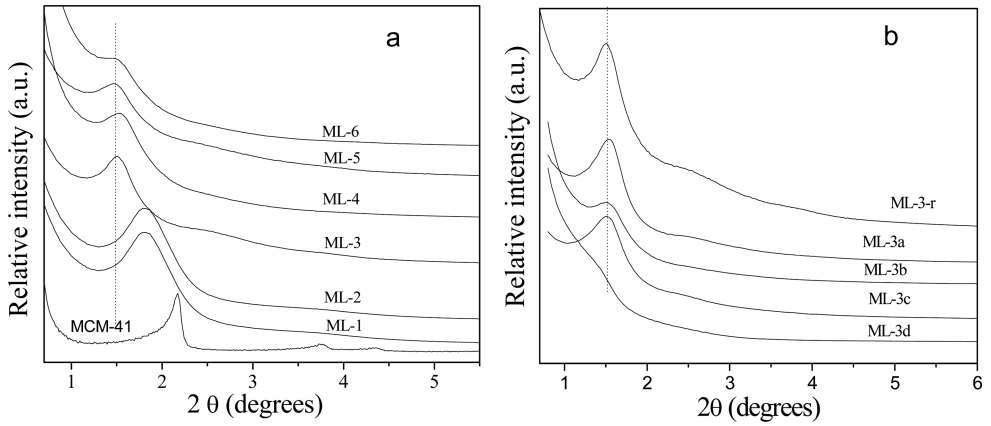

Figure 1. Low-angle XRD patterns of (a) ML-n and (b) ML-3x series samples.

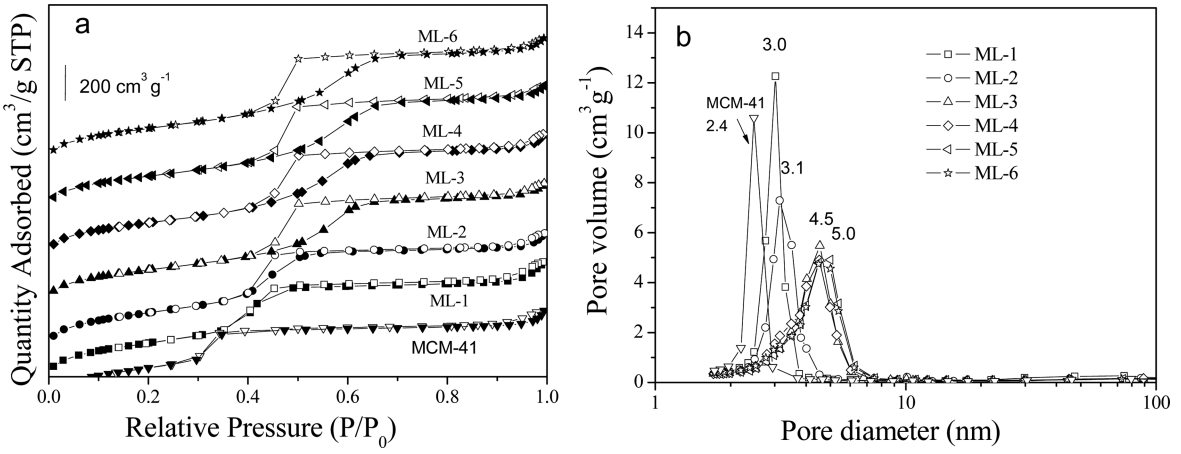

Figure 2. Nitrogen adsorption−desorption isotherms (filled points, adsorption; and open points, desorption, left) and pore size distribution (right) of ML-n samples.

STA449C apparatus in oxygen from 293 to 1073 K with a heating rate of 10 K min^{-1}. The sulfur content of composite was determined by use of a varioEL CHNS analyzer.

Detection of heparin was carried out by a colorimetric toluidine blue method[21] modified for the present study. An amount of 50 mg of heparin sodium of was dissolved in 50 mL phosphate-buffered saline (PBS) solution (pH 7.2−7.6 containing 0.02 M phosphate and 0.15 M sodium chloride) to obtain the standard heparin solution. 0.005% toluidine blue solution was prepared by adding 25 mg of *o*-toluidine blue, 2.5 mL of 2 M HCl, and 1 g of NaCl in 500 mL of distilled water. Standard heparin dilutions with concentration of 0.5, 1, 2, 4, 6, 8, 10, 12, and 14 $\mu g\ mL^{-1}$ were diluted from the standard heparin solution. Ten tubes were used for this assay. Among them, one tube was utilized as the blank. Each tube was added with 2.5 mL of toluidine blue solution, and then 2.5 mL of heparin solutions with different concentration were added to these tubes, while 2.5 mL of PBS solution was added to the blank tube. All the tubes were shaken vigorously for 30 s. Five milliliters of hexane was added to each tube and then shaken violently. This was done to extract the heparin-dye complex formed in tube 1−9. For each tube, the absorbance was measured at 620 nm using the visible spectrophotometer. A standard calibration curve was plotted by absorbance versus the heparin concentration for tube 1−10 (see Figure S1 in the Supporting Information).

Adsorption of heparin was carried out as follows: 100 mg of powderlike sample was added to a tube containing 5 mL PBS solution with 50 mg of heparin, and then the tube was kept at 277 K for 24 h. Later, the residual heparin in the solution after adsorption was measured, and the difference between this value and the original heparin concentration represented the amount of heparin to be adsorbed. Lastly, the dried powder sample after adsorption was element analyzed to determine the amount of heparin adsorbed.

After the adsorption of heparin, the sample powder was washed with 10 mL of PBS solution for three times, then the solid was put into another 10 mL of PBS solution to assess the release of heparin. The released amount of heparin at different time was determined by toluidine blue method,[21] and release profiles were obtained by plotting the time vs the release amount.

3. RESULTS

3.1. Characterization of Modified MCM-41 Composite.

Figure 1a depicts the low-angle XRD patterns of MCM-41 and ML-n samples. MCM-41 sample had a sharp characteristic peak at 2θ of 2.17 along with two peaks at 2θ of 3.74 and 4.35. ML-n samples had the weakened XRD peak as decane additive was used in synthesis. Usually, the XRD patterns of high-quality powder hexagonal mesoporous materials are characterized with four peaks with a very strong feature at a low angle of 2θ (100 reflection line) along with others at higher angles (110, 200, 210 reflection lines).[46] However, when the ratio of decane to CTAB was increased from 0 to 2.5, no secondary reflection was detected anymore on the resulting composite, and thus the regular array of channel was lost (Figure 1a). Presence of a single reflection indicated the formation of disordered structure on these samples, and the recovered mesoporous composites exhibited a wormhole-like channel system.[43] This broad peak in the XRD pattern of ML-n samples is an indication of average pore-to-pore separation in disordered wormhole framework

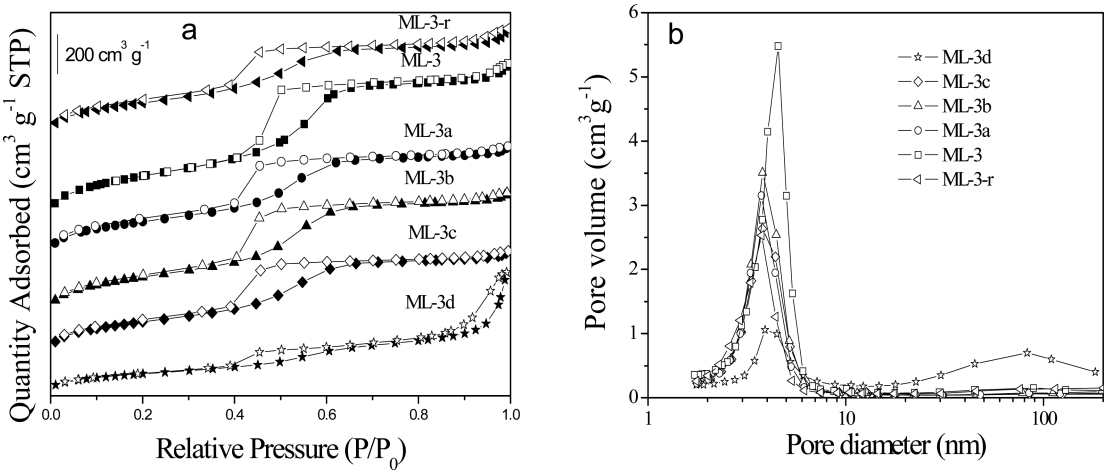

Figure 3. Nitrogen adsorption−desorption isotherms (filled points, adsorption; and open points, desorption, left) and pore size distribution (right) of ML-3x samples.

that presents a lack of long-range crystallographic order, and its shift to low degree indicates the larger pore diameter. Figure 1b displays the low-angle XRD patterns of ML-3x samples. Compared with ML-3-r, ML-3a and ML-3b samples showed similar XRD patterns but the peak gently shifted to high degree with a slightly lowered intensity. Since the reflection intensities related to the extent of pore filling and the scattering contrast between pore walls and the inside of pores,[47] such decrease of peak intensity implies less ordered structure. Sample ML-3d was synthesized with the further increased amount of APTES, and its pore order decreased intensely, because too much organic silica is not beneficial for the hydrolysis and coagulation of silica,[48] inducing the collapse of structure. In other words, organic functional group in organosilane impacts the cross-link of silica precursors, which can interrupt the pore development from micelles and cause a less-ordered mesostructure.[49] When the ratio of APTES to silica went to 0.2, ML-3d sample lost the ordered structure. Figure S2 in the Supporting Information illustrates the TEM images of ML-3 and ML-3a composites. Both samples maintain the worm-like pore structure, and the ordered degree is lowered, which complements the results obtained by XRD method.

Figure 2a illustrates the nitrogen adsorption−desorption isotherms of ML-n samples. Unlike the isotherm of MCM-41, the hysteresis loop of ML-n samples with enlarged pores was attributed to H_2 type, corresponding to ink-like or worm type pores.[50,51] Pay attention to the special point of relative pressure (P/P_0) at which the capillary condensation occurs, it can be found that this point increased from 0.3 (MCM-41) to 0.4 (ML-n, n = 1−3) when the ratio of decane to CTAB used for ML-n sample was below 1. This phenomenon indicates the expanded pore diameter caused by addition of decane. Actually the pore diameter attained a maximum on ML-3 and then kept unchanged with the further increase of decane, and the shape of hysteresis loop of ML-4, ML-5 and ML-6 was similar to that of ML-3 (Figure 2a). Decane additive has a complex influence on the pore size distribution of ML-n samples (Figure 2b). Addition of decane increased the pore size of samples as the decane/CTAB < 1, but made the pore size distribution wider once decane/CTAB > 1.

Type IV isotherm could be observed on ML-3x samples (Figure 3a), accompanied with a H_2 type hysteresis loop attributing to ink-like or worm-like pore channels. Compared with the calcined sample ML-3, these extracted samples had the hysteresis loop shifted at lower pressure region, indicating the smaller pore size caused by introduction of organic groups into channels. Different amount of organosilanes has different disruptive effects on the formation of MCM-41. According to the nitrogen adsorption isotherms of ML-3x, functionalization with amine organosiliane did not change the mesoporous structure until the ratio of APTES to silica rose to 0.2 (Figure 3a). Another hysteresis loop appeared on the isotherm of ML-3d in the region of p/p_0 = 0.9−1.0, attributing to the large accumulating pores; these pores were caused by the hydrolyzed and coagulated excessive organic silica, resulting from the detrimental effect of APTES on the meso-structure formation.[52] The pore sizes of ML-3-r and ML-3x samples (around 3.8 nm) are slightly smaller than that of ML-3 (4 nm, Figure 3b), since surface modification can cause a decrease in both pore size and BET surface area.[53] ML-3x composites, except ML-3d, have smaller surface area and pore volume than ML-3, but larger than ML-3-r sample, mirroring the complex influence of introducing organic agent on the pore structure of mesoporous silica. Besides, ML-3d also has large pores around 80 nm (Figure 3b), further verifying its disorder structure.

3.2. Adsorption of Heparin by Mesoporous Composites. Table 1 summarizes the synthetical parameter, textural property and the adsorption performance of mesoporous composites. Compared with the calcined sample MCM-41, MCM-41-r had a 30% reduced surface area and a 56% shrunk pore volume, whereas the most probable pore size decreased from 2.4 to 1.7 nm, due to the existence of residual template inside the channel[41] (about 30%, Figure S3 in the Supporting Information). Nonetheless, it adsorbed more heparin than MCM-41 did despite of its narrow pore size, demonstrating the possibility of heparin have entered into the channel with size of 1.7 nm and the promotion of retained CTAB template on the adsorption as described below. SBA-15-r sample had the surface area reduced about 87% than SBA-15, but it adsorbed more heparin (Table 1), too. These phenomena indicate the positive function of residual template micelles in the reflex sample on heparin adsorption. Especially, MCM-41-r adsorbed more heparin (65.1 mg g^{-1}) than SBA-15-r sample (34.6 mg g^{-1}) did, owing to the influence of different templates. The former contained about 30% of retained template but the latter had about 12% (see Figure S3 in the Supporting Information). As a

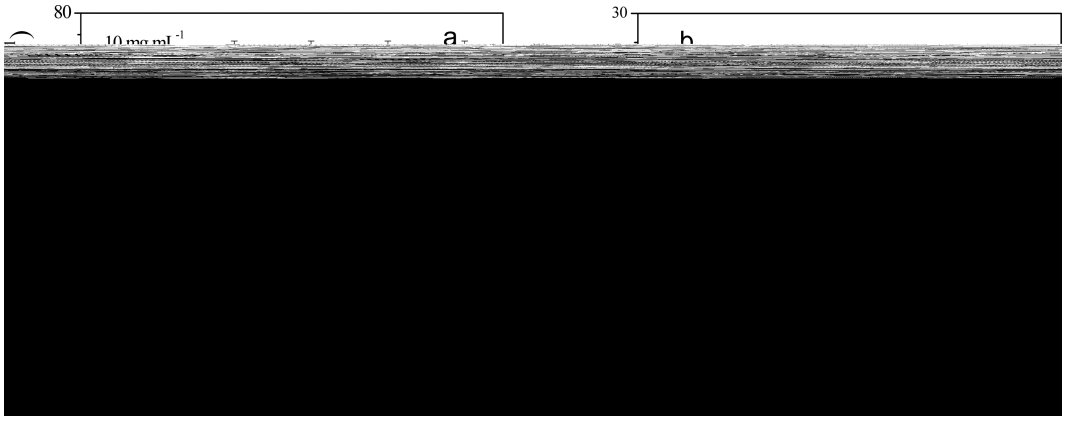

Figure 4. (a) Adsorption isotherms of heparin by the mesoporous materials at 277 K and (b) release profiles at 310 K.

Figure 5. Adsorption of heparin on MCM-41-r at (a) different concentration and (b) solution-to-solid ratio.

kind of quaternary ammonium salt with positive charge, moreover, CTAB may promote the adsorption of negative charged heparin,[54] while block copolymers P123 as the nonionic surfactant may not interact with heparin by electrostatic force. This inference is supported by the heparin adsorption on calcined sample where MCM-41 adsorbed less (14.6 mg g^{-1}) than SBA-15 (24.6 mg g^{-1}) did indeed. To identify whether heparin is adsorbed on the external surface or into the channels of MCM-41, as-MCM-41, the as-synthesized composite whose channels were occluded with template, was used to adsorb heparin, and its capacity was 6.0 mg g^{-1}. Compared with its refluxed analogue MCM-41-r with capacity of 65.1 mg g^{-1}, it appears that the external surface of MCM-41 has a minor contribution, less than one tenths, on the adsorption of heparin. To study how the adsorption of heparin affects the pore structure of these samples such as BET surface area, nitrogen adsorption experiment of ML-3 and ML-3a samples adsorbed that heparin was performed and the results were shown in Table 1 and Figure S4 in the Supporting Informaiton. Through the comparison of Figure S4 in the Supporting Information with Figure 3a, it is clear that the sample keeps the same shape isotherm after the adsorption of heparin, but the absolute value is changed. For instance, adsorption of heparin reduces the surface area of ML-3 about 55%, and the pore volume is lowered about 71%, whereas the most probable pore size decreases from 4.5 to 3.6 nm. Likewise, ML-3a after heparin immobilization has a 45% reduced surface area and a 49% shrunk pore volume but the most probable pore size kept constant. These phenomena indicate that most of the adsorbed heparin has occupied the channel of these samples.

MCM-41 and SBA-15 sample, either calcined or extracted, are utilized to explore how long is needed to achieve adsorption equilibrium of heparin in mesoporous silica (Figure 4a), and their textural properties are listed in Table 1. All samples reached the adsorption equilibrium after 2 days except for SBA-15 sample on which 3 days were needed though it adsorbed less heparin than MCM-41-r and SBA-15-r. As a result, the adsorption time in succeeding experiments is determined as 3 days.

Figure 5a displays the adsorption of heparin on MCM-41-r sample with different initial concentration. The sample showed an increased capacity of adsorption as the heparin concentration rose from 0.5 to 10 mg g^{-1}, but the proportion of heparin to be adsorbed varied irregularly, reaching maximum at the heparin concentration of 5 mg g^{-1}. In order to select the suitable liquid to solid ratio in heparin adsorption, three ratios, 15, 25, and 50 mL g^{-1}, were also tested. As can be seen in Figure 5b, the sample showed an enhanced adsorption capacity as the liquid-to-solid ratio increased while the proportion to be adsorbed varied oppositely. For the sake of maximizing the adsorbed heparin amount, we chose 10 mg g^{-1} as the

Figure 6. Release profiles of heparin on ML series samples.

experimental concentration and 50 mL g^{-1} as the solution-to-solid ratio.

Introduction of decane in synthesis successfully enlarges the pore diameter of MCM-41 (Table 1), so ML-n (n = 1−6) samples adsorbed at least 100% more heparin than MCM-41 did, and their adsorbed amount of heparin was confirmed by the TG results (see Figure S5 in the Supporting Information). Nevertheless, decane additive had a complex effect on the adsorption of heparin by ML-n sample, with the shape of volcano-type, and the higher content of decane in synthesis failed to elevate the adsorption capacity of the sample when the ratio of decane to CTAB reached 1. In the case when the pore diameters of adsorbent were similar, their adsorption ability declined with the augment of decane because of the disordered structure hence the ML-3 trapped the most heparin (54.3 mg g^{-1}) among ML-n composites. On the other hand, introduction of APTES in ML-3 sample leaded to smaller pore diameter, surface area and pore volume, but most of the ML-3x composites still adsorbed more heparin than ML-3 did (Table 1), mirroring the powerful promotion of amino groups on the adsorption of heparin. Unlike the pore-enlarged samples ML-n, ML-3x samples adsorbed more heparin as its APTES content rose hence both ML-3c and ML-3d were more active than their parent ML-3-r composite (74 mg g^{-1}) in the adsorption, adsorbing 80.4 and 99.5 mg g^{-1} of heparin, respectively.

3.3. Release of Heparin from Mesoporous Composite.

For ML-3-r, SBA-15, and MCM-41-r composites adsorbed heparin, an initial release burst occurred in the first few days (about 5 days, Figure 4b) because of the desorption of the heparin located on the external surface (about 6 mg g^{-1} for MCM-41) and near the channel mouth of the samples. After then, the release became relatively slow, in which the release, in our opinion, was a consequence of diffusion from channel. The release in the final stage, 15 days later, was rather slow and lasted until most of the encapsulated heparin desorbed. Such three-stage model is similar to that reported in literature,[55] and the last two stages may realize a sustained heparin release for the requirement of medical treatment. Both SBA-15-r and MCM-41 samples had the linear-like release profile in the beginning 15 days, and then the rate of release became rather slow (Figure 4b). All samples in Figure 4b could continue to release heparin up to 22 days, and MCM-41-r lasted for 30 days though their release amount was different. The retained template in SBA-15-r and MCM-41-r composites significantly promoted the adsorption of heparin (Table 1), but failed to improve heparin release because less than half of heparin was released.

Among MCM-41, MCM-41-r, and ML-3-r samples, ML-3-r with enlarged pore adsorbed the most heparin, and released relatively fastest. Also, the heparin release from MCM-41-r was faster than that from MCM-41 in the first 5 days. When the sample adsorbs a large amount of heparin, the concentration difference between the sample and release medium will be large, promoting heparin release while the impact of pore structure of adsorbent becomes minor. Because the release of heparin is driven by concentration difference, the more heparin adsorbed by samples, the faster they will be released into the medium. MCM-41-r adsorbed more heparin (65.1 mg g^{-1}) than MCM-41 (14.6 mg g^{-1}) did, and hence it released more heparin at the beginning, but the rate of release became slow later because of the attraction of residual CTAB template in channel. Generally speaking, two factors impact the release manners of the samples, adsorbed amount and the interaction between adsorbent and heparin. For instance, SBA-15-r adsorbed 40% more heparin than SBA-15 (Table 1) did but the H-bonding between P123 and heparin made the former to release heparin more slowly (Figure 4b).

Table 1 and Figure 6a depict the textural properties and heparin release of ML-n composite. ML-n samples can release heparin after 40 days, and among them ML-3 exhibited the largest release amount. Some samples still released a detectable amount of heparin even after 2 months. Heparin release of ML-n materials is also characterized with three-stage model and each stage is extended. Nonetheless, the heparin release of ML-3-r only lasted for 30 days, implying the negative effect of residual CTAB template in channel. Most ML-n sample had the release ratio (the release amount of heparin to the adsorbed amount) of 50%-60%, but ML-3 showed the largest of 71%. Because ML-3 has the largest adsorption capacity and release ratio (Table 1), of course its release amount is the largest. It is difficult for the heparin in the deep of channel to dissolve out hence the third release stage will last for a very long time, which is also affected by many factors such as the interaction between heparin and pore wall of adsorbent. Consequently, about two-thirds of the adsorbed heparin was slowly released (Table 1). Both pore size and pore orders of support will affect the adsorbed amount of heparin on these samples, subsequently impacting their release behavior. From ML-1 to ML-3 the pore size increases obviously, resulting in an easier and faster heparin

release; from ML-3 to ML-5 the pore size is stayed the same but pore order decreased, the release amount declined so that the released heparin obeys the order ML-1 < ML-2 < ML-6 < ML-4 < ML-5 < ML-3.

As is evident from Figure 6b, all ML-3x composites and their parent ML-3r exhibited a significant "burst effect". ML-3b and ML-3d released the same amount of heparin as ML-3-r in the first 3 days while ML-3a and ML-3c released less although ML-3c had adsorbed more heparin than ML-3-r did. Nonetheless, only ML-3d released more heparin than ML-3-r did after 10 days, and the release procedure is also consistent with the three-stage release model, with the extended time of each stage. Surface modification of MCM-41 with APTES promotes the adsorption of heparin, and more heparins are trapped by ML-3x samples with higher content of amino groups (Table 1). However, the release amount follows the order: ML-3a < ML-3c < ML-3b < ML-3-r < ML-3d. This phenomenon indicates the complex influence of organic groups on the release of heparin, and the disordered pore structure seems enabling this composite to exhibit an unexpected function in adsorbing and releasing heparin. The rough channel wall retards the movement of heparin, which may have a minor influence in the adsorption procedure because the adsorbate will be forced to move inside the inner part of channel by the obvious concentration difference between the solution and the channel, but it will be important when those heparins in the inner part of channel desorb, because their diffusion will be decelerated. Also, ML-3d sample contains some macropores (Figure 3b) and such a kind of hierarchical structure may promote the adsorption of heparin, whereas the high degree of surface roughness[56] can lead to a large fraction of inaccessible amino groups, producing a relatively weaker interaction toward heparin accompanied with the larger release amount and the more significant "burst effect" (Figure 6b). On the other hand, heparin release from ML-n and ML-3x composites could last for 2 months (Figure 6), implying their advantage in durable immobilization and sustained release of heparin. In fact, the heparin still showed the APTT value that was longer than reference (40 s) and TT value that was higher than measure limitation after released for 45 days, validating long lasting superior antithrombogenicity.[38]

To study the models of heparin release, the experimental profiles of heparin release from MCM-41 samples were fitted to theoretical models. Higuchi (1961) model,[57] $M_t/M_\infty = at^{1/2}$, and Peppas (1987) models,[23] $M_t/M_\infty = at^b$, were widely used to investigate release mechanisms.

In Higuchi formula the fraction of released drug is proportional to the square root of time; "a" is a constant, M_t and M_∞ are cumulative release amounts at time t and at infinite time, respectively. For Peppas semiempirical equation, also known as "power law", "a" is the kinetic constant and "b" is an exponent identifying the diffusion mechanism. When b = 0.5, Peppas model becomes Higuchi model. Both models are short time approximations and limited to be applied to the first 60% of release. Consequently, the release profiles in 10 days were fitted with these two models, and Table 2 shows the fitted results. Figure 7 also illustrates the fitted curves of these samples, in which the release profiles seem to be better fitted with Peppas model. Clearly the Peppas model was more suitable to fit the release profile because of the R^2 larger than 0.97, indicating good relative correlation.[58] Because Higuchi model requires the relatively unique pore properties,[58] this phenomenon implies that the samples possess the little heterogeneous pores.

Table 2. Parameters and Coefficients Obtained for Different Release Kinetic Models Fitted to the Experimental Heparin Release Profiles from MCM-41series Samples

	MCM41	MCM41-r	ML-1-r	ML-1a
Higuchi				
a	0.190	0.0910	0.117	0.0400
R^2	0.968	0.952	0.972	0.970
Peppas				
a	0.102	0.130	0.166	0.0373
b	0.823	0.302	0.308	0.552
R^2	0.998	0.974	0.976	0.972

4. DISCUSSION

Scheme 1 illustrates the chemical structure of heparin. Heparin consists of repeating disaccharide units of glucosamine and uronic acid linked by 1, 4 interglycosidic bonds.[59,60] The main functional groups in this disaccharide unit of heparin are negatively charged, such as COO−, NH−SO_3^-, O−SO_3^-, $CONHCH_3$, and OH. Therefore, positive charge can favor the adsorption of heparin. Residual template CTAB in the sample of MCM-41-r is positively charged so that it will accelerate the adsorption of heparin because the negatively charged groups of heparin will immediately bind to the positively charged CTAB. Of course, this relatively strong attraction will lead to difficulty in release as aforementioned (Scheme 2) so that 39% of the heparin adsorbed in MCM-41-r was released, less than that of MCM-41 (69%, Table 1).

Unlike ordinary small molecules like NO whose adsorption and release can be simply controlled on mesoporous silica,[61−63] biomolecule heparin has a larger volume and more complicated chemical structure so that its adsorption and release are more complex, especially on the mesoporous silica. Through the comparison of MCM-41 and some ML-n (n = 1−3) samples, pore-enlarge is beneficial for adsorption and release of heparin (Table 1). However, this modification became minor if the ML-n composites were compared with MCM-41-r; for the adsorption of heparin, the pore diameter of support has a weaker influence than the residual CTAB template (Table 1). Analogously, the surface area of mesoporous support is not vital for the adsorption and release of heparin. For instance, MCM-41 has the largest surface area among the mesoporous silica tested here, but its performance is inferior to those with smaller surface area like ML-n. The order of pore structure has a complex effect on adsorption of heparin. Some ML-n (n = 3−6) samples have the same pore size but their performance of adsorbing and releasing the biomolecule is gently lowered as more decane is used in their synthesis. This difference can be tentatively attributed to the decreased order of their pore structure. However, the adsorption capacity of this composite increases dramatically (Table 1) when macropore appears in ML-3d sample, giving a valuable clue on the function of hierarchical structure. Introduction of amino group in the mesoporous support is no doubt helpful for adsorption of heparin due to the strengthened interaction toward the biomolecule. These amine head groups on the pore wall can create a hydrophilic microenvironment, and amino group is protonated to $R_2NH_2^+$ in an aqueous medium, which makes them able to interact with negative sulfate, carboxylate, and hydroxyl groups of heparin through electrostatic interactions.[54]

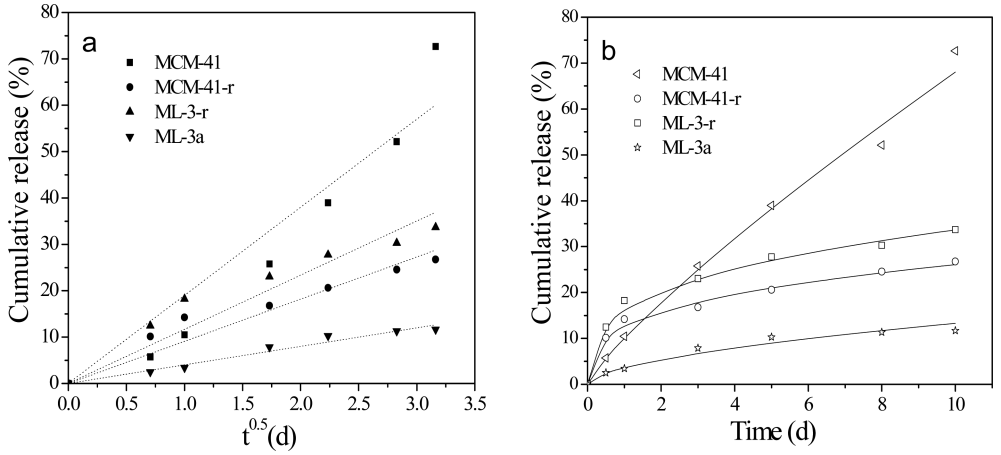

Figure 7. Release data fits to (a) Higuchi and (b) Peppas model for MCM-41 series samples.

Scheme 1. Chemical Structure of Heparin

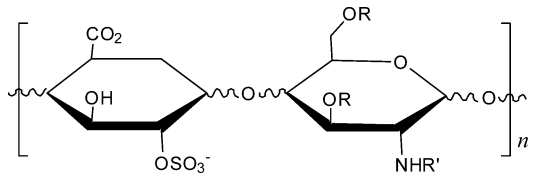

R = H or SO_3^-, R' = SO_3^- or $COCH_3$

At the same time, release of heparin is inevitably retarded because of the interaction (Scheme 2). Sample ML-3d seems to be an exception because of the existence of some macropores in the carrier (Figure 3b), and it adsorbed (99.5 mg g^{-1}) and released the largest amount (39.5 mg g^{-1}) of heparin here. Nonetheless, its relatively fast release should be ameliorated in future.

There are some discoveries based on the data in Table 1. Among various composites assessed in adsorption, MCM-41-r (65.1 mg g^{-1}), ML-3-r (74 mg g^{-1}), ML-3c (80.4 mg g^{-1}), and ML-3d (99.5 mg g^{-1}) exhibit the high capacity and they all contain organic modifier. For the release of heparin, ML-3 (38.6 mg g^{-1}) and ML-3d (39.5 mg g^{-1}) are the winners, both of them have their specialties in pore structure, ML-3 has a suitable expanded pore size while ML-3d owns a kind of hierarchical structure. Concerning the ratio of heparin adsorbed and released, the winners are SBA-15 (88%), ML-3 (71%) and MCM-41 (69%) but they contain no organic modifier. Judged from the sustained release, ML-3, ML-1 and ML-5 can keep the gently releasing over 30 days and none of them owns organic modifier. Summarizing these results, it is clear that existence of organic group in porous support will improve the adsorption of heparin but retard its release. And pore modification including proper pore expanding and introduction of macropore is beneficial for the sustain release of the biomolecule.

5. CONCLUSIONS

Different mesoporous silica materials were investigated as carriers for the controlled release of heparin, and some tentative conclusions can be drawn as follows:

(1) Mesoporous silica can adsorb and release heparin, offering the efficient carrier for long-term heparin release.
(2) Residual CTAB template in the extracted MCM-41 sample promotes the adsorption of heparin, because of the special interaction between positive charged CTAB and heparin.
(3) Proper-enlarged pore of MCM-41 is beneficial for the adsorption and release of heparin, but the ratio of decane to CTAB used in synthesis should not exceed unit in order to avoid decreasing the pore order of sample.
(4) Introduction of amino groups enhances the amount of heparin adsorbed on ML-3 samples, but slows down heparin release rate and prolongs the release time. The

Scheme 2. Possible Release Procedure of Heparin on (a) Organic-Group-Modified MCM-41 and (b) Larger-Pore MCM-41

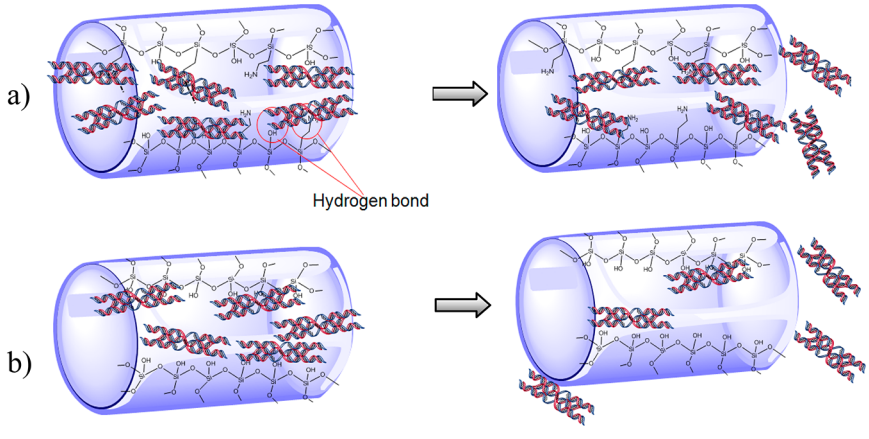

heparin encapsulated in the ML-3d composite reaches 99.5 mg g^{-1}; among them, about 40% can be released.

Although mesoporous composites markedly delay heparin release, further studies are required to identify the interaction between negative charged heparin and positive charged substances or groups such as CTAB and amino groups.

■ ASSOCIATED CONTENT

Supporting Information

The standard curve of remaining TB solution interacting with different concentrations of heparin; TG-DSC measurements of the porous samples that adsorbed heparin. This material is available free of charge via the Internet at http://pubs.acs.org/.

■ AUTHOR INFORMATION

Corresponding Author

*E-mail: jhzhu@netra.nju.edu.cn. Fax: +86-25-83317761. Tel: +86-25-83595848.

Notes

The authors declare no competing financial interest.

■ ACKNOWLEDGMENTS

NSF of China (20873059 and 21173117), Scientific Research Foundation of Graduate School, as well as Analysis Center of Nanjing University financially supported this research.

■ REFERENCES

(1) Khan, S.; Gor, J.; Mulloy, B.; Perkins, S. J. *J. Mol. Biol.* **2010**, *395*, 504−521.
(2) Sarkar, S.; Sales, K. M.; Hamilton, G.; Seifalian, A. M. *J. Biomed. Mater. Res., Part B* **2007**, *82B*, 100−108.
(3) Kidane, A. G.; Salacinski, H.; Tiwari, A.; Bruckdorfer, K. R.; Seifalian, A. M. *Biomacromolecules* **2004**, *5*, 798−813.
(4) Wang, H.; Lin, Z. X.; Liu, X. M.; Sheng, S.; Wang, J. *J. Controlled Release* **2005**, *105*, 120−131.
(5) Kazatchkine, M. D.; Fearon, D. T.; Metcalfe, D. D.; Rosenberg, D. D.; Austen, F. K. *J. Clin. Invest.* **1981**, *67*, 223−228.
(6) Sharath, M. D.; Merchant, Z. M.; Kim, Y. S.; Rice, K. G.; Linhardt, R. J.; Weiler, J. M. *Immunopharmacology* **1985**, *9*, 73−80.
(7) Folkman, J.; Langer, R.; Linhardt, R. J.; Handeschild, C.; Taylor, S. *Science* **1983**, *221*, 719−725.
(8) Crum, R.; Szabo, S.; Folkman, J. *Science* **1985**, *230*, 1375−1378.
(9) Holodniy, M.; Kim, S.; Katzenstein, D.; Konrad, M.; Groves, E. T.; Merigan, T. C. *J. Clin. Microbiol.* **1991**, *29*, 676−679.
(10) Shieh, M. T.; Spear, P. G. *J. Virol.* **1994**, *68*, 1224−1228.
(11) Capila, I.; Linhardt, R. J. *Angew. Chem., Int. Ed.* **2002**, *41*, 391−412.
(12) Liu, G.; Hultin, M.; Ostergaard, P.; Olivercrona., T. *Biochem. J.* **1992**, *285*, 731−736.
(13) Begovac, P. C.; Thomson, R. C.; Fisher, J. L.; Hughson, A.; GaÈllhagen, A. *Eur. J. Vasc. Endovasc. Surg.* **2003**, *25*, 432−437.
(14) Weber, N.; Wendel, H. P.; Ziemer, G. *Biomaterials* **2002**, *23*, 429−439.
(15) Heyligers, J. M. M.; Verhagen, H. J. M.; Rotmans, J. I.; Weeterings, C.; Groot, P. G.; Moll, F. L.; Lisman, T. *J. Vasc. Surg.* **2006**, *43*, 587−591.
(16) Yang, J.; Motlagh, D.; Allen, J. B.; Webb, A. R.; Kibbe, M. R.; Aalami, O.; Kapadia, M.; Carroll, T. J.; Ameer, G. A. *Adv. Mater.* **2006**, *18*, 1493−1498.
(17) Meng, N.; Zhang, S. Q.; Zhou, N. L.; Shen, J. *Nanotechnology* **2010**, *21*, 1−11.
(18) Saliba, M. J., Jr *Burns* **2001**, *27*, 349−358.
(19) Wendel, H. P.; Ziemer, G. *Eur. J. Cardio-thorac.* **1999**, *16*, 342−350.
(20) Li, J.; Zhu, B. Q.; Shao, Y. Y.; Liu, X. R.; Yang, X. L.; Yu, Q. *Colloids Surf., B* **2009**, *70*, 15−19.
(21) Ahola, M. S.; Sailynoja, E. S.; Raitavuo, M. H. *Biomaterials* **2001**, *22*, 2163−2170.
(22) Roveri, N.; Morpurgo, M.; Palazzo, B.; Parma, B. *Anal. Bioanal. Chem.* **2005**, *38*, 601−606.
(23) Karewicz, A.; Zasada, K.; Szxzubialka, K. *Int. J. Pharm.* **2010**, *385*, 163−169.
(24) Prabaharan, M.; Gong, S. *Carbohydr. Polym.* **2008**, *73*, 117−125.
(25) Vallet-Regí, M.; Rámila, A.; del Real, R. P.; Pérez-Pariente, J. *Chem. Mater.* **2001**, *13*, 308−311.
(26) Van der Giessen, W. J.; Lincoff, M.; Schwartz, R. S.; Van Beusekom, H. M. M.; Serruys, P. W.; Holmes, D. R.; Ellis, S. G.; Topol, E. J. *Circulation* **1996**, *94*, 1690−1697.
(27) Rechavia, E.; Litvack, F.; Fishbien, M. C.; Nakamura, M.; Eigler, N. *Cathet. Cardiovasc. Diagn.* **1998**, *45*, 202−207.
(28) Trewyn, B. G.; Giri, S.; Slowing, I. I.; Lin, V. S. Y. *Chem. Commun.* **2007**, 3236−3245.
(29) Zhu, Y. F.; Ikoma, T.; Hanagata, N.; Kaskel, S. *Small* **2010**, *6*, 471−478.
(30) Slowing, I. I.; Vivero-Escoto, J. L.; Wu, C. W.; Lin, V. S.Y. *Adv. Drug Delivery Rev.* **2008**, *60*, 1278−1288.
(31) Coti, K. K.; Belowich, M. E.; Liong, M.; Ambrogio, M. W.; Lau, Y. A.; Khatib, H. A.; Zink, J. I.; Khashab, N. M.; Stoddart, J. F. *Nanoscale.* **2009**, *1*, 16−39.
(32) Kresge, C. T.; Leonowicz, M. E.; Roth, W. J.; Vartuli, J. C.; Beck, J. S. *Nature* **1992**, *359*, 710−712.
(33) Zhao, D. Y.; Feng, J. L.; Huo, Q. S.; Melosh, N.; Fredrickson, G. H.; Chmelka, B. F.; Stucky, G. D. *Science* **1998**, *279*, 548−552.
(34) Yang, Z. L.; Lu, Y. F.; Yang, Z. Z. *Chem. Commun.* **2009**, 2270−2277.
(35) Meynen, V.; Cool, P.; Vansant, E. F. *Microporous Mesoporous Mater.* **2009**, *125*, 170−223.
(36) Munoz, B.; Ramila, A.; Perez-Pariente, J.; Diaz, I.; Vallet-Regi, M. *Chem. Mater.* **2003**, *15*, 500−503.
(37) Horcajada, P.; Rámila, A.; Férey, G.; Vallet-Regí, M. *Solid State Sci.* **2006**, *8*, 1243−1249.
(38) Zhou, Y.; Li, K.; Yang, J. Y.; Guan, C. X.; Wang, Y.; Liu, C. J.; Zhu, J. H. *Small* **2012**, *8*, 1373−1383.
(39) Lin, N.; Gao, L.; Chen, Z.; Zhu, J. H. *New J. Chem.* **2011**, *35*, 1867−1875.
(40) Wan, M. M.; Gao, L.; Chen, Z.; Wang, Y. K.; Wang, Y.; Zhu, J. H. *Microprous Mesoprous Mater.* **2012**, *155*, 24−33.
(41) Wan, M. M.; Lin, W. G.; Gao, L.; Gu, H. C.; Zhu, J. H. *J. Colloid Interface Sci.* **2012**, *377*, 497−503.
(42) Lin, H. P.; Wong, S. T.; Mou, C. Y.; Tang, C. Y. *J. Phys. Chem. B* **2000**, *104*, 8967−8975.
(43) Blin, J. L.; Su, B. L. *Langmuir* **2002**, *18*, 5303−5308.
(44) Wei, F.; Yang, J. Y.; Gao, L.; Gu, F. N.; Zhu, J. H. *J. Hazard. Mater.* **2009**, *172*, 1482−1490.
(45) Wei, Y. L.; Wang, Y. M.; Zhu, J. H.; Wu, Z. Y. *Adv. Mater.* **2003**, *15*, 1943−1945.
(46) Chen, C. Y.; Xiao, S. O.; Davis, M. E. *Microprous Mater.* **1995**, *4*, 1−20.
(47) Tkachenko, O. P.; Klemetiev, K. V.; Loffler, E.; Ritzkopf, I.; Schuth, F.; Bandyopadhyay, M.; Grabowski, S.; Gies, H.; Hagen, V.; Muhler, M.; Lu, L.; Fischer, R. A.; Grunert, W. *Phys. Chem. Chem. Phys.* **2003**, *5*, 4325−4334.
(48) Izquierdo-Barba, I.; Sousa, E.; Doadrio, J. C.; Doadrio, A. L.; Pariente, J. P.; Martínez, A.; Babonneau, F.; Vallet-Regí, M. *J. Sol−Gel Sci. Technol.* **2009**, *50*, 421−429.
(49) Hartono, S. B.; Qiao, S. Z.; Jack, K.; Ladewig, B. P.; Hao, Z.; (Max), Lu, G. Q. *Langmuir.* **2009**, *25*, 6413−6424.
(50) Grosman, A.; Ortega, C. *Langmuir* **2008**, *24*, 3977−3986.
(51) Yuan, H. K.; Ma, X. H.; Xu, Z. L. *Sci. China: Chem.* **2011**, *54*, 257−262.
(52) Maria Chong, A. S.; Zhao, X. S.; Kustedjo, A. T.; Qiao, S. Z. *Microprous Mesoprous Mater.* **2004**, *72*, 33−42.

(53) Lee, K.; Lee, D.; Lee, H.; Kim, C. K.; Wu, Z. J. *Korean J. Chem. Eng.* **2010**, *27*, 1333−1337.
(54) Tebbe, D.; Thull, R.; Gbureck, U. *Biomed. Eng.* **2007**, *6*, 1−8.
(55) Wen, L. X.; Li, Z. Z.; Zou, H. K.; Liu, A. Q.; Chen, J. F. *Pest Manage. Sci.* **2005**, *61*, 583−590.
(56) Park, K.; Lee, G. Y.; Kim, Y. S.; Yu, M.; Park, R. W.; Kim, I. S.; Kim, S. Y.; Byun, Y. *J. Controlled Release* **2006**, *114*, 300−306.
(57) Hoffart, V.; Lamprecht, A.; Maincent, P.; Lecompte, T.; Vigneron, C.; Ubrich, N. *J. Controlled Release* **2006**, *113*, 38−42.
(58) Ritter, H.; Brühwiler, D. *J. Phys. Chem. C* **2009**, *113*, 10667−10674.
(59) Roveri, N.; Morpurgo, M.; Palazzo, B.; Parma, B.; Vivi, L. *Anal. Bioanal. Chem.* **2005**, *381*, 601−606.
(60) Tebbe, D.; Thull, R.; Gbureck, U. *Acta Biomater.* **2007**, *3*, 829−837.
(61) Wei, F.; Yang, J. Y.; Hou, Q.; Zhu, J. H. *New J. Chem.* **2010**, *34*, 2897−2905.
(62) Wei, F.; Hou, Q.; Yang, J. Y.; Zhu, J. H. *J. Colloid Interface Sci.* **2011**, *356*, 526−535.
(63) Lin, W. G.; Wei, F.; Hou, Q.; Zhang, T. Y.; Zhu, J. H. *Microprous Mesoprous Mater.* **2012**, *156*, 233−243.